Influence of multiple sources on the two-neutron correlation function in Ni-induced, intermediate energy, heavy ion reactions

R. Ghetti,[1] J. Helgesson,[2] N. Colonna,[3] B. Jakobsson,[1] A. Anzalone,[4] V. Bellini,[4,5] L. Carlèn,[1] S. Cavallaro,[4,5] L. Celano,[3] E. De Filippo,[5,6] G. D'Erasmo,[3] D. Di Santo,[3] E. M. Fiore,[3] A. Fokin,[1] M. Geraci,[6] F. Giustolisi,[5,6] A. Kuznetsov,[7] G. Lanzanò,[5,6] D. Mahboub,[4] S. Marrone,[3] F. Merchez,[8] J. Mårtensson,[1] F. Palazzolo,[4] M. Palomba,[3] A. Pantaleo,[1] V. Paticchio,[3] G. Riera,[4] M. L. Sperduto,[4,5] C. Sutera,[5,6] G. Tagliente,[3] M. Urrata,[4] and L. Westerberg[9]

(CHIC Collaboration)

[1]*Department of Physics, Lund University, Box 118, SE-221 00 Lund, Sweden*

[2]*Malmö University, SE-205 06 Malmö, Sweden*

[3]*INFN and Dipartimento di Fisica, V. Amendola 173, I-70126 Bari, Italy*

[4]*INFN, Sezione di Catania, Corso Italia 57, I-95129 Catania, Italy*

[5]*Dipartimento di Fisica, Università di Catania, Corso Italia 57, I-95129 Catania, Italy*

[6]*Laboratori Nazionali del Sud (INFN), Via S. Sofia 44, I-95123 Catania, Italy*

[7]*Khlopin Radium Institute, Shvernik avenue 28, RU-194021 St. Petersburg, Russia*

[8]*Institut des Sciences Nucléaires, F-38026 Grenoble, France*

[9]*The Svedberg Laboratory, Box 533, SE-75121 Uppsala, Sweden*

(Received 19 January 2001; published 14 June 2001)

The strength of the neutron-neutron correlation function from the $E=45A$ MeV $^{58}Ni+^{27}Al$, ^{nat}Ni, and ^{197}Au reactions depends on the neutron parallel velocity. This indicates the presence of multiple sources of neutron emission. We find these sources consistent with a dissipative, binary reaction mechanism as it is described by, e.g., Boltzmann-Uehling-Uhlenbeck calculations.

DOI: 10.1103/PhysRevC.64.017602 PACS number(s): 25.70.Pq, 24.10.Nz, 29.30.Hs

During the last decade, nuclear interferometry has become an important tool for understanding not only emission time and source size in a nuclear reaction [1–3] but also many other characteristics of the emission source [4–9]. Thus nuclear interferometry allows insight into the detailed reaction mechanism and may even give information about the properties of nuclear matter. Such information puts, of course, strong constraints on theoretical models.

In actual experiments, the available space for measurements of the correlation function (CF) $C(\vec{q},\vec{P}_{tot})$, $\vec{q}=(\vec{p}_1-\vec{p}_2)/2$ and $\vec{P}_{tot}=\vec{p}_1+\vec{p}_2$, is however limited. This depends on, e.g., limited angular coverage, energy cutoffs, experimental resolution, cross-talk rejection for neutrons, etc. Another problem is the statistics that, in early experiments, only allowed to present the total CF as a function of the magnitude of the relative momentum q. More recently it became possible to obtain CF's gated on other variables, e.g., the sum of the momenta of the particle pair, P_{tot}, which is believed to distinguish between preequilibrium and equilibrium emission of particles [10–14]. There are also many other parameters that are sensitive to the different parts of the spacetime characteristics of the emission pattern [15–19]. Many theoretical models, based on quite different ingredients, can reproduce the integrated CF's, but when the additional information on gated CF's is supplied, several of them fail to reproduce the experimental data [20,21].

The purpose this Brief Report is to discuss gated CF's measured for $E=45A$ MeV ^{58}Ni-induced reactions on targets of ^{27}Al, ^{nat}Ni, and ^{197}Au [20–22]. In particular, we present the effects of neutron velocity gates on the neutron-neutron (nn) CF and give an interpretation of the results guided by Boltzmann-Uehling-Uhlenbeck (BUU) calculations [23]. After a short motivation for the choice of the BUU model and a comparison to the singles energy distributions and to the nn CF's, we discuss the nn CF sensitivity to probe that the reactions exhibit multiple sources of neutron emission.

Many recent heavy ion reaction experiments, performed with 4π detector systems, are able to map the velocity distributions of particles and fragments in a quite complete way. These experiments have demonstrated that for most heavy ion collisions in the intermediate energy regime (20–100 MeV/nucleon) the reaction mechanism is dominated by dissipative, binary collisions. A wide range of impact parameters, from quite peripheral to nearly central collisions, leads to the formation of two excited emission sources, a projectilelike source (QP) and a targetlike source (QT) [24–30]. Evidence for a third intermediate velocity source connecting QP and QT has also been reported [31–37].

Many theoretical studies based on the semiclassical BUU approach corroborate the binary character of these collisions. For example, the accurate calculations presented in Ref. [38] for the $E/A=65$ MeV $^{40}Ar+^{27}Al$ reaction, reproduce the experimental data of Ref. [25]. Also ''dynamical'' emission of light particles and intermediate mass fragments from a ''necklike'' midrapidity source is predicted by BUU [39,40].

In this work we compare experimental singles and two-neutron correlation data from $45A$ MeV ^{58}Ni-induced collisions in order to investigate if the dissipative binary collision picture can be verified. The experiment was performed at the superconducting cyclotron of Laboratori Nazionali del Sud (Catania). The neutron setup consisted of 48 BC501A liquid scintillator cylindrical cells mounted in four clusters placed 2.7 m from the target in the horizontal plane, at angular

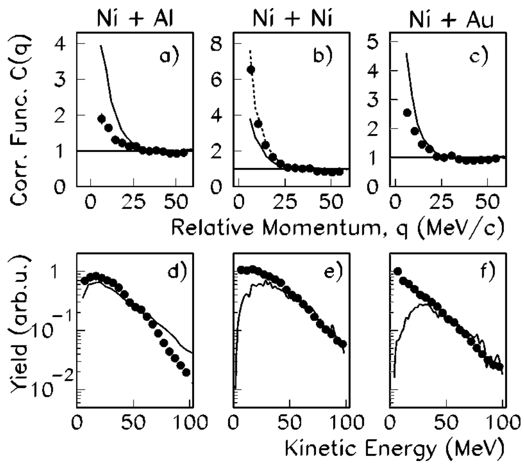

FIG. 1. Upper panels: Comparison of the experimental *nn* CF's (dots) with the theoretical CF's predicted by the BUU model for $t_{stop}=200$ fm/c (solid lines). For the Ni+Ni reaction, the BUU calculation with $t_{stop}=150$ fm/c is indicated by the dashed line in panel (b). Lower panels: Comparison of the experimental kinetic energy total yields (arbitrarily normalized) in the laboratory frame (dots), with the predictions from the BUU model (solid lines) with $t_{stop}=200$ fm/c (the experimental and BUU distributions are normalized to each other at 50 MeV).

positions of 90° and 45° on one side of the beam, 45° and 25° on the other side. Each cluster contained 12 detectors arranged in a matrix of 5×5 cells, with two consecutive detectors separated by an empty cell. A minimum separation of $\sim$4.5° between adjacent detectors was achieved in the setup. More details on the experiment can be found in [20].

First we compare the ungated *nn* CF data (previously presented in Ref. [22]) with the results of BUU calculations following the prescription of Ref. [23]. Before discussing the results, we would like to remind the reader that the reaction ^{58}Ni+^{27}Al has been extensively studied in our previous works [20,21], utilizing proton-proton (pp) and np correlation functions as well. Large set of experimental information available for this reaction allowed us to resolve some of the ambiguity of the temporal and spatial emission regions and to extract the global parameters of Gaussian radius ($R_G=2.7\pm0.3$ fm) and exponential lifetime ($\tau_n\approx600\pm200$ fm/c) for the neutron emission source. In [20] it is was also discussed that BUU is inadequate to describe the ^{58}Ni+^{27}Al reaction that is dominated by long-time emission of evaporated particles.

The experimental *nn* CF's, constructed by dividing the cross-talk rejected neutron coincidence yield by the product of two singles neutron distributions [20,21], are shown by the dots in Figs. 1(a)–(c) for the $E=45A$ MeV ^{58}Ni+^{27}Al, $^{\mathrm{nat}}$Ni, and ^{197}Au reactions. The large difference in strength of the three CF's probes the different time scale of the reactions [21]. In particular, the fact that the smallest system has the weakest correlation, indicates that the average time for the ^{58}Ni+^{27}Al collision to emit those neutrons that contribute to the small q region of the CF, must be larger than for the other reactions.

The theoretical CF's are obtained by convoluting the phase-space distribution generated with the BUU source model with the two-neutron relative wave function calculated in the framework of the Koonin-Pratt formalism [1,2]. In the BUU simulations the two colliding nuclei are initialized in their ground states. The phase-space distribution of the source function is represented by 500 ''test particles'' per nucleon that propagate in a density dependent mean field. In addition, nucleon-nucleon collisions with Pauli blocking are included. For all three targets the BUU calculations are performed with a geometrical averaging over the appropriate range of impact parameters, a density cutoff value of 0.02 fm^{-3} and a cutoff time $t_{stop}=200$ fm/c to stop the calculations. The time of 200 fm/c is chosen after verifying that a shorter time would miss some of the particles emitted at the end of the fast dynamical processes (such as preequilibrium and neck emission). A longer stopping time would allow classical evaporation to be taken into account. However, the onset of this effect is rather slow and for instance a stopping time of 300 fm/c would only slightly modify the results obtained with 200 fm/c. A Skyrme parametrization of the nuclear potential is used, with the mean field given by $U=-124(\rho/\rho_0)+65(\rho/\rho_0)^2+U_{Coloumb}$ (MeV). For each neutron pair emitted from the source, a weight is calculated, taking into account antisymmetrization and final state interactions of the neutrons. The CF is then constructed by summing over all pairs. All theoretical calculations are filtered through the experimental energy thresholds, energy and position resolution and detector efficiencies. Furthermore, all background corrections (in particular the cross-talk rejection) are incorporated into the calculations in exactly the same fashion as in the data analysis [21,22].

Figures 1(a),(c) show that the BUU CF's have too large strength as compared to the experimental data for ^{27}Al and ^{197}Au targets. To understand this, it should be kept in mind that, due to our choice of the stopping time, the calculations presented in Fig. 1 all lack the contribution from evaporation; this leads to an underestimation of the low part of the energy spectra and to an artificial enhancement of the CF strength. A shorter stopping time would lead to even stronger correlation functions, while a longer stopping time would eventually lead to weaker correlations. However, we believe that at these bombarding energies, BUU describes fairly well the gross features of the initial stages of the collision (including preequilibrium and neck emission), but it is inappropriate to describe the later evaporative stages.

The experimental singles kinetic energy distributions (dots) are compared with the BUU calculations (lines) in Figs. 1(d)–(f). Since evaporation of particles from the excited projectile and target residues is not included in the BUU calculations (which stop before full equilibrium is reached) and since no ''afterburner'' is introduced, one should expect the low energy evaporative particles to be missing. This is indeed observed for the direct kinematics reactions [Figs. 1(e),(f)]. For the reverse kinematics ^{58}Ni+^{27}Al collision, BUU also overpredicts the high energy tail [Fig. 1(d)]. This is because in reverse kinematics the lack of evaporative particles affects a broader range of energies.

The comparison with the ^{58}Ni+$^{\mathrm{nat}}$Ni CF data is different, as the BUU calculation rather underpredicts the CF strength [Fig. 1(b)]. This indicates that the late evaporative stage is less important for this symmetric reaction. The height of the experimental ^{58}Ni+^{nat}Ni CF is better reproduced if a shorter stop time ($t_{stop}=150$ fm/c) is introduced [dashed line in Fig. 1(b)]. The corresponding energy distribution is nearly unchanged (and therefore it is not plotted in Fig. 1(e)].

In light of recent experimental findings [32–37], the differences between the three reactions may be connected to the different importance of dynamical emission of neutrons from the highly excited midvelocity source created in the overlap region. This midrapidity source emission is thought to be strongly influenced by dynamical effects, including preequilibrium and neck emission [39,40], and to occur on a short time scale. Our data suggest that for the asymmetric reaction systems, QP and QT evaporative emission is most important, while for ^{58}Ni+^{nat}Ni reactions the midrapidity source is present and even dominates. This interpretation, already put forward in [22] from the analysis of high P_{tot}-gated CF's, is strengthened also in the study of the gated CF's presented below.

In 4π detector experiments the different sources of particle emission can be identified reasonably well by means of invariant cross section contour plots in the $v_\parallel$-$v_\perp$ space. If, however, only a limited angular coverage is achieved, it can be harder to deduce the sources directly from such contour plots. Guided by the BUU results, it may still be possible to define gates on the particle velocity that will enhance or suppress a particular source. Thus, the QP source will be enhanced by demanding a high neutron parallel velocity in the laboratory system and suppressed by applying the opposite cut (low parallel velocity).

For the three different reactions that we have studied, the experimental filter provides different coverage of the various emission sources. Yet, the BUU simulations show that for all three reactions, a selection of high neutron parallel velocities favors the QP source. As demonstrated by the BUU dynamical analysis performed in [38], this QP portion of phase-space is ''contaminated'' by particles promptly emitted from the overlapping zone between the two colliding partners. In order to suppress this contamination, we select neutron pairs with low total momentum in the center-of-mass frame (P_{tot} <270, 210, and 180 MeV/c for ^{27}Al, ^{nat}Ni, and ^{197}Au targets). This slightly suppresses the experimental CF's [star symbols in Figs. 2(a)–(c)] as compared to the ungated ones (solid dots). The effect is somewhat stronger for the ^{58}Ni +^{nat}Ni reaction, where the midrapidity source contamination is presumably larger.

The next step is to introduce a selection of neutrons with high parallel velocity. In this way, emission from the QP source should be enhanced. Guided by the BUU results, neutrons with lab velocities $v_\parallel>0.12c$, $0.11c$, and $0.10c$ for ^{27}Al, ^{nat}Ni, and ^{197}Au targets, are selected. This gives the experimental CF's indicated by the open squares in Figs. 2(d)–(f). One can notice a clear enhancement in the CF strength for both ^{nat}Ni and ^{197}Au targets, while the effect is much weaker for the ^{27}Al target. The complementary gate (i.e., selection of neutrons with small parallel velocity, $v_\parallel$ $<0.11c$, $0.10c$, and $0.07c$ for ^{27}Al, ^{nat}Ni, and ^{197}Au targets) yields a slight suppression of the CF's [open circles in Figs. 2(d)–(f)] similar to the results of the selection of small total

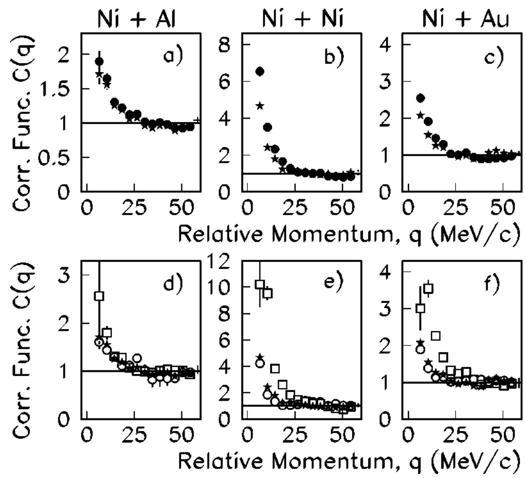

FIG. 2. Experimental nn CF's for the three targets. Upper panels: ungated CF's (solid dots) and low P_{tot}-gated CF's (stars). Lower panels: low P_{tot}-gated CF's (stars), compared to: low P_{tot}– high $v_\parallel$-gated CF's (open squares) and low P_{tot}– low $v_\parallel$-gated CF's (open circles). The values of P_{tot} and $v_\parallel$ utilized to define the cuts are indicated in the text.

momentum. This may be expected, as the low $v_\parallel$ cut implies inclusion of a larger number of uncorrelated neutron pairs (coming from different sources) and consequently a suppression of the CF strength.

The CF enhancement for high $v_\parallel$ neutrons, observed in all three cases, is most likely due to an enhanced presence of neutrons from the midrapidity source. An alternative interpretation of the results may however exist. Namely, the very small effect of the $v_\parallel$ cuts for the ^{58}Ni+^{27}Al system [Fig. 2(d)] could indicate that the QT and the QP sources have similar excitation energies. This interpretation would be in agreement with the results of the BUU theoretical calculations of Ref. [38] and also with a recent experimental study of the $E=44A$ MeV ^{40}Ar+^{27}Al reaction [41]. In [38] as well as in [41] it is suggested that this reaction is of binary nature and that the two excited nuclei (QT and QP) that emerge from the collision have very similar, and quite low, temperatures. The clear enhancement of the QP-CF observed for the ^{58}Ni+^{197}Au collision [Fig. 2(f)] could instead indicate a higher excitation of the QP source as compared to the QT source. Finally, the strong CF enhancement, observed for the ^{58}Ni+^{nat}Ni symmetric system (especially with a high $v_\parallel$ cut) would indicate the presence of a stronger midrapidity source component (as suggested also by the comparison of integrated CF's with BUU calculations in Sec. II B).

The parallel velocity cuts applied to the data have been applied also to the BUU calculations. In contrast to the experimental results, no noticeable effects on the CF strength have been observed. This may well be expected, since the evaporative stage is missing in the BUU calculations. However, it also seems to indicate that, while BUU describes fairly well the geometrical aspects of the sources, it does not equally well describe the details of the spacetime characteristics of the nucleon emission.

In this Brief Report we have compared the ungated neutron-neutron CF measured for the reactions E

$=45A$ MeV ^{58}Ni+^{27}Al, ^{nat}Ni, and ^{197}Au, with the CF gated on the neutron parallel velocity, and we have discussed the experimental results in terms of multiple-source emission as suggested by BUU calculations. While the BUU model can reproduce some of the integrated CF's, it cannot reproduce the significant change in CF strength experimentally observed when the parallel velocity cuts are applied. Thus $v_{\parallel}$-gated CF's constitute a new, additional constraint for theoretical models.

The authors wish to thank Bao-An Li and W. Bauer for making their BUU code available. G. Antuofermo, G. Iacobelli, M. Sacchetti, P. Vasta, A. Masciullo, G. Poli, N. Guardone, and V. Sparti are thanked for technical support and the LNS accelerator crew for providing a high quality beam. Financial support from the ''Knut och Alice Wallenberg'' and ''Helmuth Hertz'' Foundations is gratefully acknowledged by R.G. The support from the Swedish Natural Science Research Council is appreciated.

[1] S.E. Koonin, Phys. Lett. **70B**, 43 (1977).
[2] S. Pratt and M.B. Tsang, Phys. Rev. C **36**, 2390 (1987).
[3] D.H. Boal, C.K. Gelbke, and B.K. Jennings, Rev. Mod. Phys. **62**, 553 (1990).
[4] W.G. Gong *et al.*, Phys. Rev. C **47**, R429 (1993).
[5] D.O. Handzy *et al.*, Phys. Rev. C **51**, 2237 (1995).
[6] L. Martin *et al.*, Nucl. Phys. **A583**, 407 (1995).
[7] D. Ardouin, Int. J. Mod. Phys. E **6**, 391 (1997).
[8] P.A. DeYoung *et al.*, Phys. Rev. C **56**, 244 (1997).
[9] P.A. DeYoung *et al.*, Phys. Rev. C **61**, 024603 (2000).
[10] M.A. Lisa *et al.*, Phys. Rev. Lett. **70**, 3709 (1993).
[11] M. Cronqvist *et al.*, Phys. Lett. B **317**, 505 (1993).
[12] S.J. Gaff *et al.*, Phys. Rev. C **52**, 2782 (1995).
[13] P.A. DeYoung *et al.*, Nucl. Phys. **A597**, 127 (1996).
[14] S.J. Gaff *et al.*, Phys. Rev. C **54**, 2161 (1998).
[15] D. Rebreyend *et al.*, Phys. Rev. C **46**, 2387 (1992).
[16] M.A. Lisa *et al.*, Phys. Rev. Lett. **71**, 2863 (1993).
[17] M.A. Lisa *et al.*, Phys. Rev. C **49**, 2788 (1994).
[18] D.O. Handzy *et al.*, Phys. Rev. C **50**, 858 (1994).
[19] N. Colonna *et al.*, Phys. Rev. Lett. **75**, 4190 (1995).
[20] R. Ghetti *et al.*, Nucl. Phys. **A660**, 20 (1999).
[21] R. Ghetti *et al.*, Nucl. Phys. **A674**, 277 (2000).
[22] R. Ghetti *et al.*, Phys. Rev. C **62**, 037603 (2000).
[23] W. Bauer, Nucl. Phys. **A471**, 604 (1987); B.-A. Li and W. Bauer, Phys. Rev. C **44**, 450 (1991); Bao-An Li (private communication).
[24] J.F. Lecolley *et al.*, Phys. Lett. B **325**, 317 (1994).
[25] J. Peter *et al.*, Nucl. Phys. **A593**, 95 (1995).
[26] R. Bougault *et al.*, Nucl. Phys. **A587**, 499 (1995).
[27] Y. Larochelle *et al.*, Phys. Lett. B **352**, 8 (1995).
[28] M.F. Rivet *et al.*, The INDRA Collaboration, Phys. Lett. B **388**, 219 (1996).
[29] W. Skulski *et al.*, Phys. Rev. C **53**, R2594 (1996).
[30] O. Dorvaux *et al.*, Nucl. Phys. **A651**, 225 (1999).
[31] C.P. Montoya *et al.*, Phys. Rev. Lett. **73**, 3070 (1994).
[32] Y. Larochelle *et al.*, Phys. Rev. C **55**, 1869 (1997).
[33] J. Lukasik *et al.*, The INDRA Collaboration, Phys. Rev. C **55**, 1906 (1997).
[34] P. Pawloswki *et al.*, Phys. Rev. C **57**, 1771 (1998).
[35] G. Lanzanò *et al.*, Phys. Rev. C **58**, 281 (1998).
[36] Y. Larochelle *et al.*, Phys. Rev. C **59**, R565 (1999).
[37] E. Plagnol *et al.*, The INDRA Collaboration, Phys. Rev. C **61**, 014606 (1999).
[38] Ph. Eudes, Z. Basrak, and F. Sébille, Phys. Rev. C **56**, 2003 (1997).
[39] M. Colonna, M. di Toro, V. Latora, and A. Smerzi, Prog. Part. Nucl. Phys. **30**, 17 (1992); M. Colonna, M. Di Toro, and A. Guarnera, Nucl. Phys. **A589**, 160 (1995); M. Colonna, M. Di Toro, A. Guarnera, V. Latora, A. Smerzi, and Z. Jiquan, *ibid.* **A583**, 525c (1995); M. Colonna, M. Di Toro, A. Guarnera, S. Maccarone, M. Zilinska-Pfabé, and H.H. Wolter, *ibid.* **A642**, 449 (1998); G. Fabbri, M. Colonna, and M. Di Toro, Phys. Rev. C **58**, 3508 (1998).
[40] L. Sobotka, Phys. Rev. C **50**, R1270 (1994); L. Sobotka, J.F. Dempsey, R.J. Charity, and P. Danielewicz, *ibid.* **55**, 2109 (1997).
[41] G. Lanzanò *et al.*, Nucl. Phys. **A683**, 566 (2001).